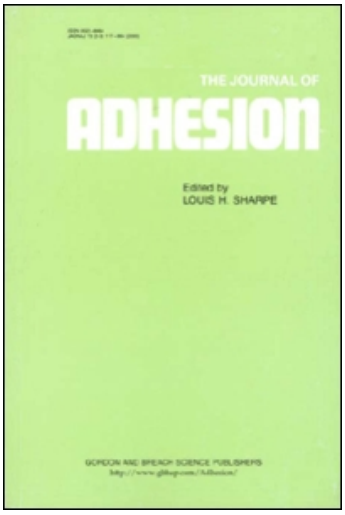

The Journal of Adhesion

Publication details, including instructions for authors and subscription information:
http://www.informaworld.com/smpp/title~content=t713453635

Crack Path Selection in Adhesively-Bonded Joints: The Role of Material Properties

Buo Chen[ab]; David A. Dillard[a]; John G. Dillard[c]; Richard L. Clark Jr.[de]

[a] Engineering Science and Mechanics Department, Virginia Polytechnic Institute and State University, Blacksburg, Virginia, USA [b] Cooper Tire & Rubber Company, Findlay, OH, USA [c] Chemistry Department, Virginia Polytechnic Institute and State University, Blacksburg, Virginia, USA [d] Materials Science and Engineering Department, Virginia Polytechnic Institute and State University, Blacksburg, Virginia, USA [e] College of the Canyons, Santa Clarita, CA.

To cite this Article Chen, Buo , Dillard, David A. , Dillard, John G. and Clark Jr., Richard L.(2001) 'Crack Path Selection in Adhesively-Bonded Joints: The Role of Material Properties', The Journal of Adhesion, 75: 4, 405 — 434
To link to this Article: DOI: 10.1080/00218460108029613
URL: http://dx.doi.org/10.1080/00218460108029613

J. Adhesion, 2001, Vol. 75, pp. 405–434
Reprints available directly from the publisher
Photocopying permitted by license only

Crack Path Selection in Adhesively-Bonded Joints: The Role of Material Properties

BUO CHEN [a,*], DAVID A. DILLARD [a,†], JOHN G. DILLARD [b] and RICHARD L. CLARK JR. [c,‡]

[a]*Engineering Science and Mechanics Department,* [b]*Chemistry Department,* [c]*Materials Science and Engineering Department, Virginia Polytechnic Institute and State University, Blacksburg, Virginia 24061, USA*

(Received 15 January 2000; In final form 30 October 2000)

This paper investigates the role of material properties on crack path selection in adhesively bonded joints. First, a parametric study of directionally unstable crack propagation in adhesively-bonded double cantilever beam specimens (DCB) is presented. The results indicate that the characteristic length of directionally unstable cracks varies with the Dundurs' parameters characterizing the material mismatch. Second, the effect of interface properties on crack path selection is investigated. DCB specimens with substrates treated using various surface preparation methods are tested under mixed mode fracture loading to determine the effect of interface properties on the locus of failure. As indicated by the post-failure analyses, debonding tends to be more interfacial as the mode II fracture component in the loading increases. On the other hand, failures in specimens prepared with more advanced surface preparation techniques appear more cohesive for given loading conditions. Using a high-speed camera to monitor the fracture sequence, DCB specimens are tested quasi-statically and the XPS analyses conducted on the failure surfaces indicate that the effect of crack propagation rate on the locus of failure is less significant when more advanced surface preparation techniques are used. The effect of asymmetric interface property on the behavior of directionally unstable crack propagation in adhesive bonds is also investigated. Geometrically-symmetric DCB specimens with asymmetric surface pretreatments are prepared and tested under low-speed impact. As indicated by Auger depth profile results, the centerline of the crack trajectory shifts slightly toward the interface with poor adhesion due to the asymmetric interface properties. Third, through varying the rubber content in the adhesive, DCB

*Present address: Cooper Tire & Rubber Company, 701 Lima Avenue, Findlay, OH 45840, USA.
†Corresponding author: Tel.: 540-231-4714, e-mail: dillard@vt.edu
‡Present address: College of the Canyons, Santa Clarita, CA.

specimens with various fracture toughnesses are prepared and tested. An examination of the failure surfaces reveals that directionally unstable crack propagation is more unlikely to occur as the toughness of the adhesive increases, which is consistent with the analytical predictions that were discussed using an energy balance model.

Keywords: Directional stability of cracks; Locus of failure; Surface pretreatment; Crack path selection; Adhesively bonded joints; T-stress; Interfacial failure; Cohesive failure; Mixed mode fracture

INTRODUCTION

Cracks and flaws are inevitable in manufacture and service life of adhesively-bonded joints and propagation of the cracks will greatly reduce the life of the joints and may cause unexpected failure. Therefore, understanding the crack propagation behavior is an important aspect in evaluating the performance of adhesively-bonded joints. For a crack located within the adhesive layer, the crack propagation behavior is closely related to the stress state at the crack tip [1–4]. If a Cartesian coordinate is set at the crack tip with x-axis pointing along the crack plane, the stress distribution at the crack tip can be expressed by Williams' asymptotic stress expansion [5],

$$\begin{bmatrix}\sigma_{xx} & \sigma_{xy}\\ \sigma_{xy} & \sigma_{yy}\end{bmatrix} = \frac{K_I}{\sqrt{2\pi r}}\cos\left(\frac{\theta}{2}\right)\begin{bmatrix}1-\sin\left(\frac{\theta}{2}\right)\sin\left(\frac{3\theta}{2}\right) & \sin\left(\frac{\theta}{2}\right)\sin\left(\frac{3\theta}{2}\right)\\ \sin\left(\frac{\theta}{2}\right)\sin\left(\frac{3\theta}{2}\right) & 1+\sin\left(\frac{\theta}{2}\right)\sin\left(\frac{3\theta}{2}\right)\end{bmatrix} + \frac{K_{II}}{\sqrt{2\pi r}}\begin{bmatrix}-\sin\left(\frac{\theta}{2}\right)\left[2+\cos\left(\frac{\theta}{2}\right)\cos\left(\frac{3\theta}{2}\right)\right] & \cos\left(\frac{\theta}{2}\right)\left[1-\sin\left(\frac{\theta}{2}\right)\sin\left(\frac{3\theta}{2}\right)\right]\\ \cos\left(\frac{\theta}{2}\right)\left[1-\sin\left(\frac{\theta}{2}\right)\sin\left(\frac{3\theta}{2}\right)\right] & \sin\left(\frac{\theta}{2}\right)\cos\left(\frac{\theta}{2}\right)\cos\left(\frac{3\theta}{2}\right)\end{bmatrix} + \begin{bmatrix}T & 0\\ 0 & 0\end{bmatrix} + O(\sqrt{r}) \tag{1}$$

where r and θ are the polar coordinates and K_I and K_{II} are the mode I and mode II stress intensity factors, respectively. The third term in Eq. (1) is non-singular and acts parallel to the crack plane. By convention, this term is referred to as the "T-stress". In order to obtain an overall understanding of the crack propagation behavior, knowledge of K_I, K_{II}, and T is essential since they characterize the stress state at the crack tip [1, 2, 6–10].

For cracks in brittle homogeneous materials, the stress intensity factors K_I and K_{II} characterize the singular stresses at the crack tip and, therefore, are closely associated with the onset of fracture and the direction of cracking [1, 11]. More specifically, the onset of fracture for brittle materials is characterized by the critical mode I fracture toughness, K_{Ic}, according to the conventional theory of fracture. The direction of cracking, as indicated by Goldstein and Salganik [11], Cotterell and Rice [1] and Hutchinson and Suo [2], is related to the fracture mode mixity characterized by the phase angle, Ψ, which is defined as

$$\Psi = \tan^{-1}\left(\frac{K_{II}}{K_I}\right) \tag{2}$$

The direction of crack propagation can be determined using the mode I fracture criterion [11], which states that a crack will propagate in a direction such that pure mode I fracture is maintained at the crack tip, *i.e.*, $K_{II} = 0$ or $\Psi = 0$ at the advancing crack tip.

Although the criteria for the onset of fracture and the direction of cracking were developed for homogeneous materials, they can be readily extended to bi-materials systems such as adhesively-bonded joints [2]. However, when the crack is at the bi-material interface, care should be used when applying the mode I fracture criterion for direction of cracking due to differences in fracture toughness in the vicinity of an interface as indicated in Refs. [12] and [13]. Chen and Dillard [12] provided an example showing how to use these criteria to determine the direction of cracking when the crack is located at the interface.

According to the mode I fracture criterion for the direction of cracking, in testing adhesive bonds, the locus of failure is predicted to be closely associated with the mode mixity of the loading. As the mode

II fracture components in the loading increase, failure tends to be more interfacial. By loading DCB specimens in mixed mode fashion and conducting X-ray photoelectron spectroscopy (XPS) and Auger depth profile analyses on the failure surfaces to identify the locus of failure, Chen *et al.* [10] demonstrated the mode mixity dependence of the locus of failure in adhesive bonds. The discussions in Ref. [10] mainly focused on the effect of external loads and specimen geometry. However, according to Refs. [14–17], the surface morphology and chemistry of adherends can be altered using different surface preparation methods. As a result, the quality of adhesion for a particular materials system can be greatly enhanced if appropriate surface pretreatment is used. Therefore, the locus of failure or other crack propagation behavior under certain loading conditions might also be altered significantly due to the changes in the interface properties, which suggests that an investigation of the effect of interface properties on crack path selection in adhesive bonds is necessary.

The T-stress in Eq. (1) is a non-singular stress acting parallel to the crack plane and is relatively small in the vicinity of the crack tip as compared with the singular terms in the equation. In investigating slightly curved or kinked cracks under mode I loading, Cotterell and Rice [1] indicated that the T-stress plays an important role in the directional stability of crack propagation. The crack trajectory is directionally stable if the T-stress is negative, whereas the crack trajectory is directionally unstable if the T-stress is positive.

In adhesively bonded joints, the issue of directional stability of cracks was first discussed by Chai [18], who observed a unique alternating crack trajectory in testing graphite-reinforced epoxy composite laminates and aluminum/epoxy bonds under mode I fracture loading. Fleck, Hutchinson and Suo [4] and Akisanya and Fleck [6, 7] investigated this directional stability issue analytically and indicated that as with homogeneous materials, the directional stability of cracks in adhesively-bonded joints also depends on the T-stress level. By testing symmetric double cantilever beam (DCB) specimens with various levels of the T-stresses, Chen and Dillard [13] demonstrated that the crack trajectory was relatively straight when the T-stress is negative (compressive) and is alternating when the T-stress positive (tensile). These results verify the T-stress dependence of the directional stability of cracks in adhesive bonds.

Based on an energy balance idea, Chen and Dillard [12] constructed an analytical model using an idealized crack trajectory resembling the "square wave" to predict the crack propagation manner in adhesively bonded DCB specimens. The result of the analysis is shown in Figure 1. The ordinate of the figure is the normalized average strain energy release rate according to the critical strain energy release rate G_c ($=310\,J/m^3$) of the DCB specimens tested in Ref. [13], and the abscissa represents the thickness of the adherends. The dashed line represents the critical strain energy release rate for the alternating crack propagation and, therefore, also represents the threshold of the transition of the directional stability of the crack propagation. If the available strain energy release rate is higher than the critical strain energy release rate for the alternating crack trajectory, cracks in the specimen are more likely to be directionally unstable since there is more than enough energy available for cracks to propagate along the alternating path. On the other hand, if the available strain energy release rate for the alternating crack propagation is lower than the critical strain energy release rate, cracks are more likely to be directionally stable. Figure 1 shows the results of the analysis for the DCB specimens tested in Ref. [13]. The specimens had a thermal

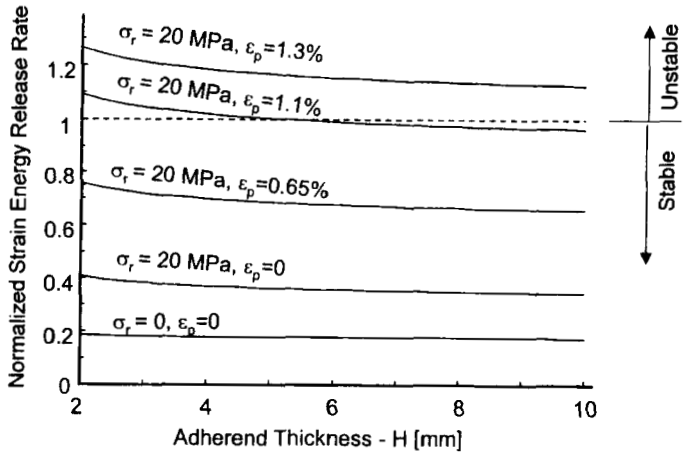

FIGURE 1 The directional stability of cracks in DCB specimens predicted using the energy balance model in Ref. [12]. The strain energy available is normalized to $G_c = 310\,J/m^2$.

residual stress of $\sigma_0 = 13$ MPa induced from curing. Before testing, the specimens were stretched mechanically until the adherends were plastically deformed to alter the residual stress and, consequently, the T-stress in the specimens [13]. Figure 1 shows that when the plastic deformation in the adherends, ε_p, is less than 1.1%, the curves are all below the dashed line indicating a likelihood for directionally stable crack propagation. As the plastic deformation, ε_p, in the adherends increases (consequently, the T-stress also increases), more and more strain energy becomes available and the curves shift upwards, suggesting an increase in the probability of directionally unstable cracks. This result is consistent with the predictions made by Fleck, Hutchinson and Suo [4] using the T-stress argument. Experimental results discussed in Ref. [13] also indicated good consistency with the predictions made by the energy balance model.

The energy balance model also predicted an effect of the toughness of adhesive bonds on the probability of the directional stability of cracks. As shown in Figure 1, if the toughness of the bonds, G_c, increases, all the curves will shift downward vertically and the transition between directionally stable and unstable crack propagation is less likely to occur. Since the toughness of adhesive bonds varies significantly with the material system, an investigation of the effect of the fracture toughness of the adhesive bonds on the directional stability of cracks can provide important insight into the general understanding of the crack path selection behavior in adhesively-bonded systems.

With knowledge of the criteria for the direction of crack propagation and interface mechanics, the crack trajectories for directionally unstable crack propagation can be predicted [12]. Compared with the experimentally-observed alternating crack trajectory as shown in Ref. [12], the predicted trajectory accurately simulated the alternating features of the crack such as the characteristic length and the overall shape.

As suggested by the "shear-lag" concept for adhesively-bonded single-lap joint specimens, one can predict from the results in Ref. [12] that the alternating nature of the crack is closely related to the material mismatch of the system and can be explained using a model analogous to the "shear-lag". For a bi-material system, the material mismatch is characterized by the Dundurs' parameters α and β, which are defined

as

$$\alpha = \frac{\mu_1(\kappa_2 + 1) - \mu_2(\kappa_1 + 1)}{\mu_1(\kappa_2 + 1) + \mu_2(\kappa_1 + 1)}$$
$$\beta = \frac{\mu_1(\kappa_2 - 1) - \mu_2(\kappa_1 - 1)}{\mu_1(\kappa_2 + 1) + \mu_2(\kappa_1 + 1)} \tag{3}$$

where the subscripts 1 and 2 refer to the materials for the adherends and adhesive, respectively; μ_i $(i = 1, 2)$ are shear moduli; $\kappa_i = 3 - 4\nu_i$ for plane strain and $\kappa_i = (3 - \nu_i)/(1 + \nu_i)$ for plane stress; and ν_i $(i = 1, 2)$ are the Poisson's ratios. The value of α is between -1 and 1, and according to Suga *et al.* [19] and Hutchinson and Suo [2], the value of β is between 0 and $\alpha/4$ for most material combinations.

This paper focuses on the effect of material properties on the crack path selection in adhesively-bonded joints. First, directionally unstable crack trajectories in DCB specimens of different material systems were simulated using the finite element method and the characteristic length of the cracks was demonstrated to be dependent on the material mismatch. Second, the effect of the interface properties on the locus of failure was investigated. DCB specimens with adherends treated by different surface preparation methods were tested in mixed mode fracture fashion. Post-failure analyses including XPS and Auger depth profiling were conducted to identify the locus of failure. The results indicate that the locus of failure, while strongly dependent on the fracture mode mixity, is also closely related to the interface properties. Third, the effect of surface preparation on the rate dependence of the locus of failure in adhesively-bonded specimens was studied. DCB specimens with various T-stress levels and surface pretreatments were tested quasi-statically and the fracture sequence was recorded using a high-speed camera. XPS analysis of the failure surfaces indicated that the effect of debond rate on the locus of failure was less significant as the surface preparation was improved. Fourth, DCB specimens with asymmetric surface pretreatments were tested to investigate the effect of interface asymmetry on crack propagation behavior. As indicated by the Auger depth profile data, an asymmetric crack trajectory resulted due to the interface asymmetry. Last, by varying the rubber content in the adhesive, DCB specimens with different fracture toughnesses were

obtained and the effect of adhesive toughness on the directional stability of cracks was studied. The examination of the failure surfaces revealed that directionally unstable crack propagation was more unlikely to occur as the toughness of the adhesive increased, which was consistent with the predictions made in Ref. [12] using the energy balance model.

FRACTURE ANALYSIS

A Parametric Study of Directionally Unstable Crack Propagation

In this section, a parametric study of the characteristic length of directionally unstable cracks in DCB specimens of different materials systems was conducted using the finite element method. The finite element packages used were ABAQUS® [20] and FRANC2DL [21]. The 2-D model analyzed in ABAQUS® was a typical DCB geometry with dimensions shown in Figure 2. A straight interfacial crack with an idealized kink was included in the geometry, simulating the alternating behavior for a directionally unstable crack. The objective of the analysis was to predict the crack propagation behavior after kinking. At the right end of the model, the displacements were totally constrained and at the left end, two constant loads were applied. One load was applied horizontally to maintain a positive T-stress level in the model and the other load was applied vertically to simulate the external loading. The deformed finite element mesh around the crack tip is shown as the insert in Figure 2; eight-node, plane-strain elements were used with reduced integration and quarter-point singular elements were constructed around the crack tip. Both adherends and adhesive were modeled as linear elastic materials with various Young's modulus combinations characterized by Dundurs' parameter, α, to simulate the materials mismatch for different materials systems. The Poisson's ratio for both materials was estimated as $\nu_1 = \nu_2 = 0.33$. Therefore, according to Eq. (3), $\beta = 0.247\alpha$ under plane-strain conditions.

From the finite element analysis, the stress distributions ahead of the crack tip ($\theta = 0$) were obtained, which, according to Williams [22],

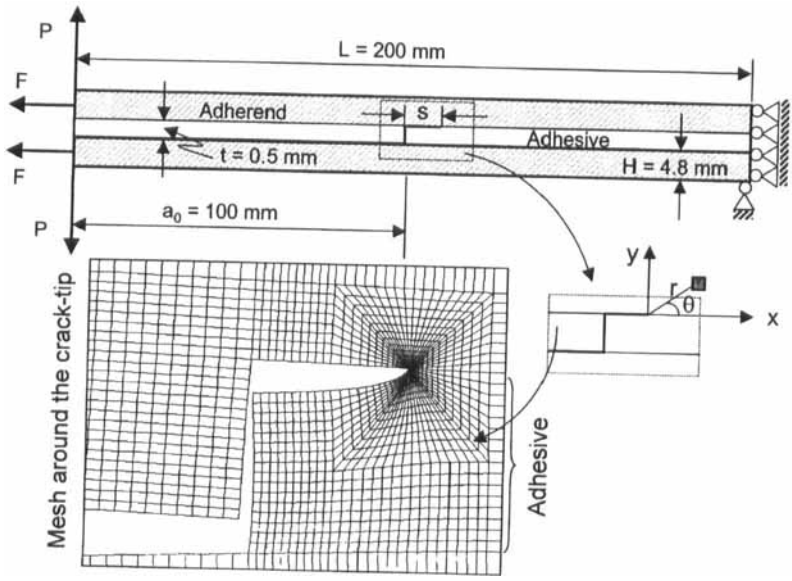

FIGURE 2 The DCB specimen geometry used in the finite element analysis to determine the crack propagation behavior after the kinking occurred. The insert is the mesh around the crack-tip.

have the general form of

$$\sigma_{yy} + i\sigma_{xy} = \frac{(K_1 + iK_2)r^{i\varepsilon}}{\sqrt{2\pi r}} \tag{4}$$

where $(r^{i\varepsilon}/\sqrt{r}) = (1/\sqrt{r})\cos(\varepsilon \ln r) + i(1/\sqrt{r})\sin(\varepsilon \ln r)$ is the oscillatory singularity characteristic of cracks at the interface between two dissimilar solids, K_1 and K_2 are the complex stress intensity factors, analogous to the conventional stress intensity factors K_I and K_{II}, and ε is defined as

$$\varepsilon = \frac{1}{2\pi}\ln\left(\frac{1-\beta}{1+\beta}\right) \tag{5}$$

Due to the oscillatory nature in the stress ahead of the crack tip, the local fracture mode mixity and direction of cracking are relatively difficult to determine for interfacial cracks. According to Hutchinson, Mear and Rice [23], Suo and Hutchinson [24] and Hills *et al.* [25], the solution for an interfacial crack can be approached by the solution for

a sub-interface crack, which lies a small distance, δt, below the interface, as the distance between the crack and the interface decreases to zero. Dattaguru *et al.* [26] verified this argument numerically using finite element analysis. By investigating the global energy balance, Hutchinson, Mear and Rice [23] and Suo and Hutchinson [24] also obtained the relationship between the complex stress intensity factors K_1 and K_2 for the interfacial crack and the conventional stress intensity factors K_I and K_{II} for the corresponding sub-interface crack as

$$K_I + iK_{II} = qe^{i\phi}(K_1 + iK_2)\delta t^{i\varepsilon} \tag{6}$$

where $q = \sqrt{(1-\beta^2)/(1+\alpha)}$ is a real quantity, and $\phi(\alpha, \beta)$ is a dimensionless function listed by Hutchinson and Suo [2] for different materials combinations. With Eq. (6), the mode mixity at the interface crack tip can be expressed in terms of the conventional definition of the phase angle Ψ as

$$\Psi = \tan^{-1}\left(\frac{K_{II}}{K_I}\right) = \tan^{-1}\left(\frac{\mathrm{Im}[(K_1 + iK_2)\delta t^{i\varepsilon}]}{\mathrm{Re}[(K_1 + iK_2)\delta t^{i\varepsilon}]}\right) + \phi \tag{7}$$

Numerically, by knowing the stress distributions ahead of the interfacial crack tip, the right parts of Eq. (7) can be determined by fixing the value of δt [6]. According to Refs. [23] and [26], the analytical result for a sub-interface crack converges quickly as the sub-interface crack approaches the interface. Slight variation of δt will only induce negligible error. For the convenience of comparison, in this study, δt is chosen to be 1 μm. From Ψ obtained using Eq. (7), the direction of crack propagation can be inferred using the mode I fracture criterion for the direction of cracking.

Analysis Results

Figure 3 shows the analysis results for the phase angle, Ψ, *versus* the normalized kink crack length with respect to the adhesive thickness. Each curve in the figure corresponds to a particular material combination characterized by the Dundurs' parameter α ($\beta = \alpha/4$). Take the curve with $\alpha = 0.92$ as an example to explain the crack

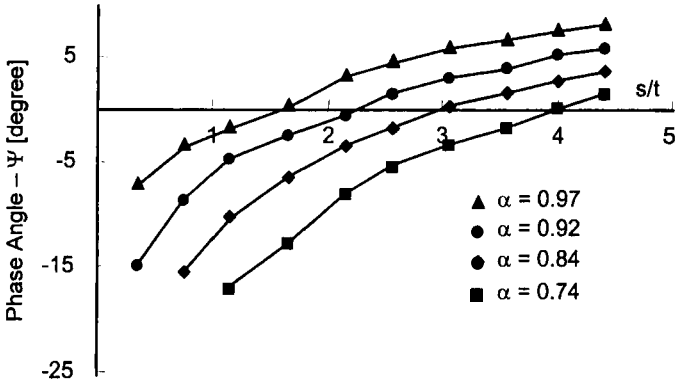

FIGURE 3 The phase angle at the crack tip *versus* the normalized kinked crack length, s/t, for different materials combinations obtained from the parametric study.

propagation behavior since the curve corresponds to the aluminum/epoxy system studied in Refs. [10, 12] and [13] and in this paper. The phase angle is negative when the crack length is small, which, according to the mode I fracture criterion, indicates that the direction of cracking is towards the adherend. However, since the adherends normally are much tougher than the adhesive for joints such as the aluminum/epoxy system studied, the direction of cracking is then restricted to the interface. As the crack length increases, the figure shows that the phase angle also increases and finally becomes positive when $s/t > 2.2$. Since the direction of cracking corresponding to a positive phase angle is towards the adhesive, the crack is forced to deviate from the interface after the sign of the phase angle changes. This transition of the direction of cracking with the crack length finally results in an alternating crack trajectory with a characteristic length ranging from 3–4 times the thickness of the adhesive layer. This range of the characteristic length was determined in the analysis using meshes with different density. This prediction is consistent with the experimental observations and the numerical simulation results of the crack trajectory in Ref. [12]. Similar behavior was also found for the T-stress. After the crack kinked into the interface, the T-stress at the crack tip was relatively small ($\cong 0$). Similar to the "shear-lag" situation in an adhesively-bonded single-lap joint specimen, the T-stress also increased as the crack continued to propagate along the interface until the kinked crack length approached the characteristic

length, at which point the crack became directionally unstable and deviated away from the interface. Therefore, the characteristic length of the crack is closely related to the characteristic length of the "shear-lag" model for the T-stress.

If the material system changes, for instance if steel is used for the adherend instead of aluminum in the DCB specimens, the material mismatch factor, α, becomes 0.97 and Figure 3 shows that the curve shifts left. As a result, the sign change of the phase angle (or the direction of cracking) occurs at a smaller crack length ($s/t \cong 1.7$) and, consequently, the characteristic length for directionally unstable cracks is predicted to be smaller. On the other hand, if a low modulus material is used for the adherends, α decreases and Figure 3 shows that the curve shifts right, indicating a larger characteristic length in the crack propagation.

To demonstrate further the effect of material properties on the characteristic length of the directionally unstable crack propagation, numerical simulations of the crack propagation using FRANC2DL were also conducted. An adhesive layer (material 2) with thickness of $t = 0.5\,\text{mm}$ is sandwiched between two adherends (material 1) with thickness of $H = 6\,\text{mm}$, and a straight crack with a small crack perturbation at the tip is located at the interface between the adhesive and the adherend. The displacements of one end of the model were constrained. Moments of opposite direction were applied on the other end of the adherends to simulate the external loads. A horizontal tensile stress, T^{∞}, was applied to achieve the desired T-stress level. Three types of elements were used in the analysis. Eight-node, plane-strain elements were used with reduced integration in the area away from the crack tip; right around the crack tip, the elements used were quarter-point singular elements; and in the area in between, triangle elements were used for the convenience of remeshing during the crack propagation. Both the adherends and adhesive were modeled as linear elastic materials with various material combinations characterized by the Dundurs' parameter, α. The residual stress in the adhesive layer was estimated as 13 MPa and the adhesive bond was assumed to have an iso-fracture toughness value of $310\,\text{J/m}^2$. The interface crack with a small perturbation was assumed to be present originally in the specimen and T^{∞} was adjusted to such a value that $K_{II} = 0$ at the crack tip. This analysis was intended to predict the crack trajectory as the crack advances through the following procedure:

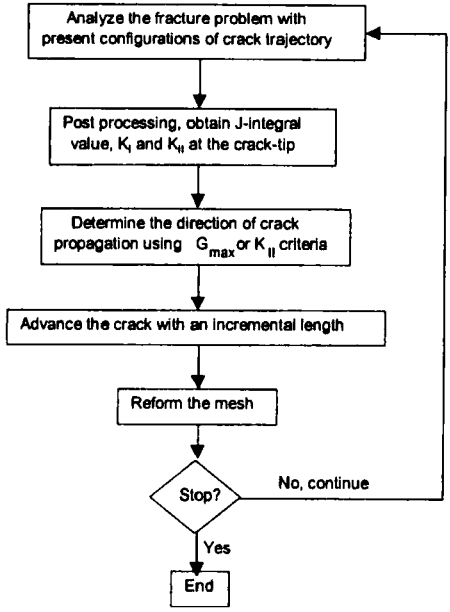

Further details of the mesh constructions, boundary conditions, and the calculation scheme in the simulation can be found in Ref. [12]. Only the final results are reported here. The crack trajectories obtained from the numerical simulation for different material combinations are shown in Figure 4. The FEA meshes are hidden to observe the crack

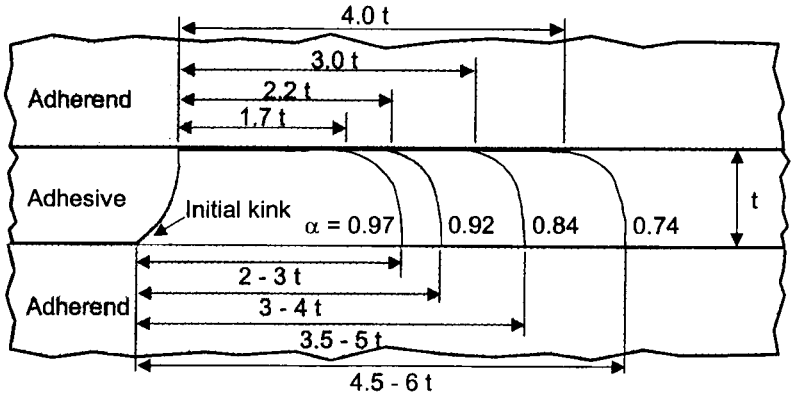

FIGURE 4 The crack trajectories of directionally unstable crack propagation for different materials systems predicted using the finite element analysis.

trajectories more clearly. The figure shows that the crack trajectories for different material combinations are all self-similar in shape; however, the characteristic length decreased as the Dundurs' parameter, α, increased.

MATERIALS AND EXPERIMENTS

To investigate the effect of material properties on the crack path selection in adhesively-bonded joints, both symmetric ($h = H$, where h and H are the thicknesses of the upper and lower adherends, respectively.) and asymmetric ($h \neq H$) double cantilever beam (DCB) specimens with various adhesive and adherend thickness were prepared and tested in this study. The width of the specimens was 25.4 mm, the length was 200 mm, and the thickness of the adhesive layer was controlled to be 0.5 mm. The adhesive used was Dow Chemical epoxy resin D.E.R. 331 mixed with a M-5 silica filler, a dicyandiamide ("DICY") curing agent, a tertiary amine accelerator (PDMU), and a rubber toughener (Kelpoxy G272-100). The details of the adhesive formulation procedure can be found in Vrana *et al.* [27]. The final products, according to the rubber concentration level, were designated as adhesive A (0% rubber), B (4.1%), C (8.1%), and E (15%). Adherends were aluminum 6061-T6 alloy. Before bonding, the surfaces of the adherends were treated with three different kinds of surface preparation methods: acetone wipe, which was used simply to provide surface uniformity among specimens; base-acid etch, and P2 etch. The base-acid etch procedure is a deep cleaning procedure, and after the preparation a new aluminum oxide surface was generated [14, 15]. The treatment was carried out by immersing aluminum in 5% (weight ratio) aqueous sodium hydroxide solution at 50°C for 5 min; rinsing the specimen in DI water; neutralizing residual surface sodium hydroxide in dilute nitric acid; rinsing the adherend in DI water again; air drying the specimen; and placing the adherend in a desiccator until bonding was carried out. The P2 surface treatment was employed to develop a robust oxide surface and avoid the use of toxic chromium(VI). In the procedure an Fe(III) solution was used to oxidize the aluminum surface. The P2 etch method, according to Wegman [14, 16], can greatly improve the surface morphology and

chemistry of the aluminum substrates and, therefore, can significantly improve adhesion. The specimens were cured at 170°C for 90 minutes, cooled to room temperature, and then stored in a desiccator prior to testing.

The material properties of the cured adhesive were characterized using differential scanning calorimetry (DSC) (for the glass transition temperature, T_g), thermal mechanical analysis (TMA) (for coefficient of thermal expansion (CTE), α_2), and room temperature dogbone tensile tests (for the Young's modulus, E_2). The results shown in Table I indicate that as the rubber concentration increases, the CTE of the material increases but the modulus and the glass transition temperature decrease slightly. To simplify the analysis, the Poisson's ratio for all the adhesives was estimated as $\nu_2 = 0.33$ at room temperature. The material properties for the aluminum 6061-T6 substrate are Young's modulus, $E_1 = 70\,\text{GPa}$, Poison's ratio, $\nu_1 = 0.33$, and CTE, $\alpha_1 = 26 \times 10^{-6}/°\text{C}$.

Due to the mismatch of the coefficients of thermal expansion, an equal bi-axial residual stress, σ_0, was induced throughout the adhesive layer after curing of the specimens. If the adherends are assumed to be relatively thick and rigid as compared with the adhesive, the residual stress is then given by

$$\sigma_0 = \frac{E_2}{1 - \nu_2}(\alpha_2 - \alpha_1)(T_{\text{sft}} - T_t) \tag{8}$$

T_{sft} in Eq. (8) is the stress-free temperature of the adhesive, which was measured using a curvature measurement technique for each adhesive [28] and was very close to the glass transition temperature (the results are also listed in Tab. I); T_t is the testing temperature (room temperature in this study). Since the coefficients of thermal expansion

TABLE I Material characterization results of the epoxy adhesive formulations used in the study

Adhesive designation	*Rubber concentration*	*CTE* ($10^{-6}/°C$)	T_g (°C)	*Modulus (GPa)*	*Calculated residual stress (MPa)*
A	0%	58	125	3.10	14.8
B	4.1%	59.5	119	3.06	14.38
C	8.1%	62	112	2.97	13.8
E	15.0%	65	106	2.85	13.4

of the adhesives increased with rubber concentration and, meanwhile, the modulus and the glass transition temperature decreased slightly, as shown in Table I, the calculated residual stresses induced in the specimens during the curing were very similar for all the adhesives. On the other hand, as will be discussed later, the rubber toughener enhanced the fracture toughness of the adhesive bonds significantly.

To alter the T-stress levels in the specimens, the DCB specimens were mechanically stretched in a universal testing machine uniaxially as discussed in Ref. [13] until the substrates were plastically deformed. An extensometer was attached to the specimens to monitor the strain. Due to the plastic deformation, ε_p, in the adherends, the residual stress in the specimen was increased and is given by [29]

$$\begin{aligned} \sigma_{xx} &= \sigma_0 + \frac{E_2}{1-\nu_2^2}(1-\nu_1\nu_2)\varepsilon_p \\ \sigma_{yy} &= \sigma_0 + \frac{E_2}{1-\nu_2^2}(\nu_2-\nu_1)\varepsilon_p \end{aligned} \tag{9}$$

where σ_0 is the thermal residual stress induced by the curing procedure of the adhesive bonds. Due to increase in the residual stress, the T-stress was also increased and the final state of the T-stress was calculated using the finite element method for different testing geometries. Details of the calculations can be found in Ref. [13].

The fracture testing and post-failure analysis methods used in this paper are quasi-static DCB tests, low-speed impact tests on DCB geometry [10], and end notch flex (ENF) tests [30]. After failure, post-failure analyses including X-ray photo-electron spectroscopy (XPS), scanning electron microscopy, and Auger depth profiling were conducted on the failure surfaces to determine the locus of failure. All the testing methods and post-failure analysis procedures were introduced in Ref. [10] and further details can be found in the literature referenced in Ref. [10].

TEST RESULTS AND DISCUSSION

Surface Preparation and Mixed Mode Fracture Tests

To investigate the effect of surface preparation on the locus of failure in adhesive bonds under mixed mode fracture tests, both quasi-static

DCB and ENF tests were conducted on specimens with adherend surfaces prepared with acetone wipe, base-acid etch, and P2 etch. The adhesive used was adhesive C and all the specimens tested were as-produced with negative T-stress levels [13]. For the ENF tests, specimens were symmetric and for the DCB tests, specimens were both symmetric and asymmetric with three different adherends thickness ratios, *i.e.*, $h/H = 0.5$, 0.75 and 1, which give rise to a fracture mode mixity of $\psi = 22°$, 10°, and 0°, respectively [10]. The failure surfaces were first examined visually, and one typical specimen was selected from each test for subsequent XPS and Auger depth profiling to identify the locus of failure. The XPS analysis was carried out on two representative areas on both the aluminum and the adhesive sides of each failed specimen. On the other hand, the Auger depth profiling was only conducted on two small areas on the aluminum side of the failure surfaces. For both tests, only the average values are reported in this paper.

Table II shows the XPS results for each test. Five elements, carbon, aluminum, nitrogen, silicon, and oxygen were detected on the failure surfaces and their concentrations varied with the testing conditions. Since the major sources for each element are already clear [10], variations in the concentrations of these elements imply changes in the locus of failure in the specimens. Carbon is the major element of the epoxy adhesive; nitrogen is from the DICY curing agents and is usually present on the surface at a very low level; silicon is from the filler; and aluminum is exclusively from the aluminum adherend. Although both the adhesive and the aluminum surface contain oxygen, the oxygen concentration in the aluminum oxide layer is much higher. According to Table II, the carbon concentration in the failure surfaces of the symmetric DCB specimens is very high while the aluminum concentration is apparently below the detection limit of the XPS (about 0.2%). As the fracture mode mixity increases, the carbon concentration on the failure surfaces decreases while the aluminum and oxygen concentrations increase. On the failure surfaces of the ENF specimens, the aluminum and oxygen concentrations are relatively high and the carbon concentration is relatively low. In addition, this carbon is unlikely from the epoxy according to its chemical nature shown in the XPS spectrum, but is more likely from the air contamination or aluminum extrusion. Since the high

TABLE II The XPS elemental analysis results for typical specimens selected from each test. The adherends of the specimens were prepared using an acetone wipe, a base/acid etch, or the P2 etch

Analysis results		*Test method*			
		Symmetric DCB ($h/H=1$)	*Asymmetric DCB* ($h/H=0.75$)	*Asymmetric DCB* ($h/H=0.5$)	*ENF*
Ψ (degree)		0	10	22	90
$G_{II}/G\%$		0	3	14	100
C%	Acetone	76.4	76.3	53.0	44.5
	B/A	76.5	76.5	73.1	45.5
	P2	76.4	76.4	74.0	52.8
Al%	Acetone	0.2	0.3	9.3	14.8
	B/A	0.3	0.5	1.9	13.7
	P2	0.1	0.2	0.4	9.1
O%	Acetone	18.7	18.8	31.8	36.7
	B/A	18.6	17.9	19.0	34.4
	P2	18.8	18.5	18.1	31.9
N%	Acetone	2.6	2.5	2.6	2.0
	B/A	2.4	2.7	2.0	2.4
	P2	2.7	2.6	3.0	2.6
Si%	Acetone	2.1	2.3	3.6	2.0
	B/A	2.2	2.4	4.0	4.0
	P2	2.0	2.0	4.5	36

aluminum and oxygen concentrations suggest the failure location is within the aluminum oxide layer, these results indicate that failure tended to be more interfacial as the mode mixity increased as discussed in Ref. [10].

On the other hand, as the surface preparation method varies, the element concentrations, especially for carbon and aluminum, also vary significantly in the tests with mode mixity G_{II}/G higher than 14%, and the trend of the variation suggests an effect of interface properties on the locus of failure. For instance, when a more advanced surface preparation method was used, the carbon and silicon concentrations increased and the aluminum and oxygen concentrations decreased. These results suggest that advanced surface preparation methods enhance adhesion and displace failure from the interface.

To quantify the locus of failure further, the epoxy film thicknesses on the failure surfaces of each specimen were measured. On the failure surfaces of the specimens tested under mode I loading or under mixed mode loading with a phase angle of 10°, a visible layer of adhesive was

observed. For these specimens, a Nikon Measurescope 2305 was used to measure the epoxy film thickness. On the other hand, for the specimens tested under mode II loading or under mixed mode loading with a phase angle of 22°, the failure surfaces appeared to be clear, which indicates that the failure occurred at or near the interface. The Auger depth profiling method was then used for those specimens, which appeared to fail interfacially.

As shown in Table III, in the mode I test, the thicknesses of the residual adhesive layers on the failure surfaces were about 250 μm for all the specimens with different surface preparations, which indicated that the failures all occurred in the middle of the adhesive layer in the test regardless of the surface preparation method since the total thickness of the adhesive of the specimens was 500 μm. When the phase angle increased as in the asymmetric DCB test with $h/H = 0.75$, which contains 3% of mode II fracture component, a layer of epoxy film with a thickness of around 50 μm was detected on the failure surfaces of all the specimens. Although the failure was still cohesive, the decrease in the film thickness on the metal side of the failure surfaces indicated that the locus of failure shifted toward the interface due to the increase in the mode mixity. On the other hand, because the failure was still cohesive, no significant effect of interface properties on the locus of failure was observed. When the mode mixity increased to 14% as in the asymmetric DCB test with $h/H = 0.5$, where the mode mixity strongly forced the crack toward the interface, the effect of interface properties on the locus of failure became pronounced. In the specimen with adherends prepared with acetone wipe, a 4 nm thick

TABLE III The Auger depth profile results for typical specimens selected from each test. The adherends of the specimens were prepared using an acetone wipe, a base/acid etch, or the P2 etch

		Test method			
Analysis results		*Symmetric DCB* ($h/H = 1$)	*Asymmetric DCB* ($h/H = 0.75$)	*Asymmetric DCB* ($h/H = 0.5$)	*ENF*
Ψ (degree)		0	10	22	90
G_{II}/G(%)		0	3	14	100
Depth profile	Acetone	250 μm	50 μm	4 nm	3.5 nm
	B/A	250 μm	55 μm	12 nm	6 nm
	P2	250 μm	57 μm	100 nm	26.5 nm

epoxy film was detected on the failure surfaces; in the specimen with adherends treated with base/acid etch, the film thickness was 12 nm; and in the P2 etched specimen, a visible layer of film, which was estimated to be about 100 nm, was observed on the failure surfaces. This increasing trend in the measured film thickness from the failure surfaces suggested that the advanced surface preparation methods enhance adhesion and displace failure from the interface, which also confirmed the indications obtained from the XPS analyses. In the ENF test, a similar trend in the variation of film thickness was observed.

The XPS and the Auger depth profile analyses clearly identify the locus of failure and verify the analytical prediction made by applying the criteria of direction of cracking to adhesive bonds. Through the testing of specimens prepared by different surface preparation techniques, these results also demonstrated the effect of interface properties on the locus of failure and verify that crack path selection in adhesive bonds is a result of interactions between external loads and material properties [9]. The results also indicated that since the locus of failure is very sensitive to the interface properties in the asymmetric DCB tests with fracture mode mixity of 14% or higher, the asymmetric DCB test can be employed rather than the ENF test to evaluate the interface fracture properties in adhesively-bonded joints. Since the asymmetric DCB test is conducted under predominantly opening mode, the onset of fracture and the crack propagation sequence are much easier to observe; this substitution can greatly simply the testing procedure. Other details of asymmetric DCB analysis and testing can be found in Refs. [31] and [32], where the fracture behavior of asymmetric DCB specimens prepared using adherends of dissimilar materials were particularly discussed.

Surface Preparation and the Rate Dependence of the Locus of Failure

In Ref. [10], the rate dependence of the locus of failure in adhesive bonds was studied. The adhesive was adhesive C and the adherends were prepared by acetone wipe before bonding. The post-failure analysis results showed that when the T-stress was negative, the failures were all cohesive and the cracks were directionally stable regardless of the debond rate; as the T-stress increased, the cracks

became directionally unstable and a very pronounced effect of debond rate on the locus of failure was observed. The failure was more interfacial when the debond rate was low. To investigate the influence of the interface properties on the rate dependence of the locus of failure in specimens with high T-stresses, two groups of symmetric DCB specimens with adherend surfaces prepared using either an acetone wipe or P2 etch were prepared and tested under quasi-static loading condition. A Kodak EktaPro high-speed camera system was used in the same manner as in Ref. [10] to monitor the fracture sequence and to obtain the rate of crack propagation. After failure, a representative specimen from each group of specimens was selected based on visual examination for the XPS analyses to identify the locus of failure.

In Figure 5, the failure surfaces of the two representative specimens are shown. The adherend surfaces of specimen (a) were prepared using an acetone wipe, and a P2 etch was used in preparing the substrates for specimen (b). The T-stresses in both specimens were 35 MPa and the magnitude of the crack propagation rates for different regions of the specimens, which were obtained using the high-speed camera, were

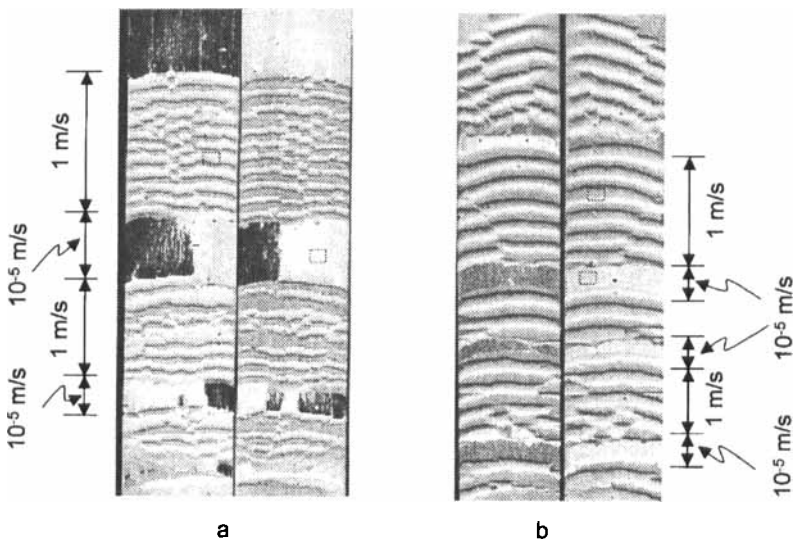

FIGURE 5 The failure surfaces of the DCB specimens prepared using acetone wipe (a) and P2 etch (b). The ⋯ indicates the areas where XPS analyses were conducted.

marked along both specimens to quantify the effect of debond rate. Through visual examination of the failure surfaces of specimen (a) and (b), the influence of surface preparation on the rate dependence of the locus of failure can be observed. In specimen (a), in the region of slow crack propagation, the failure surface was clear, indicating interfacial failure. On the other hand, in the region of fast crack propagation, the failure appeared to be cohesive since a visible layer of adhesive film was observed on the failure surface. However, in specimen (b), the difference in the locus of failure between the slow and fast crack propagation regions was not as pronounced. As a matter of fact, a visible layer of adhesive film was observed in both regions. Another noticeable difference in the failure surfaces between specimen (a) and (b) is that the regions of slow crack propagation in specimen (b) were considerably smaller than in specimen (a), indicating that the rate dependence of the locus of failure was significantly reduced due to the variation in interface properties.

The XPS analyses were conducted on the areas in both the slow and fast crack propagation regions of each specimen as schematically shown in Figure 5. The XPS data further identified the locus of failure and supported the results of visual examinations. As shown in Table IV, for specimen (a), the major element concentrations on the failure surfaces, especially carbon and aluminum, varied significantly between the slow and the fast crack propagation regions and indicated that the failure was more interfacial in the region of slow crack propagation. On the other hand, for specimen (b), although the variations of the major element concentrations between the slow and the fast regions also indicated a similar trend in the rate dependence of the locus of failure, the magnitude of the variation suggested that this debond rate effect in specimen (b) was not as pronounced as in specimen (a).

TABLE IV The XPS elemental analysis results of the symmetric DCB specimens with either an acetone wipe or the P2 etch surface preparation

Specimen	*Surface treatment*	*Region analyzed*	*XPS atomic percentage*				
			C%	*Al%*	*O%*	*N%*	*Si%*
A	Acetone	Fast	76.1	0.4	16.8	2.5	4.3
		Slow	72.3	2.1	20.9	2.6	2.1
B	P2	Fast	76.5	0.2	16.9	4.3	2.1
		Slow	75.9	0.9	15.7	4.1	3.4

Overall, the comparison of the rate dependence of the locus of failure between the two representative specimens with different surface preparations revealed that the interface properties significantly affect the crack propagation behavior. Advanced surface preparation techniques enhance the adhesion between the adhesive and the substrates and, consequently, the rate dependence of the locus of failure is reduced.

Figure 5 also shows that the characteristic length of the crack propagation in specimen (a) is smaller than that in specimen (b), indicating an influence of interface properties. As discussed in the analytical section of this paper, the characteristic length of the crack varies with the material mismatch factors α and β. Figure 5 suggests that because the more advanced surface preparation technique was used in preparing specimen (b), the adhesion was improved and consequently, the material mismatch in the vicinity of the interface was also altered as compared with specimen (a). Since in the alternating crack propagation the failure occurred at or near the interface, different characteristic lengths of the crack resulted between specimens (a) and (b).

Asymmetric Surface Preparation and the Directionally Unstable Cracks

In Ref. [10], the effect of mixed mode fracture on the directional stability of cracks was studied. Asymmetric DCB specimens with different adherend thickness ratios were tested. The results showed that the direction of crack propagation is stabilized very rapidly as the mode mixity increases; when the mode mixity, G_{II}/G, is more than 3%, cracks in the specimens were all directionally stable regardless of the T-stress levels. In this study, the effect of asymmetric surface preparation on the directionally unstable cracks is of interest. Geometrically-symmetric DCB specimens with one adherend prepared using an acetone wipe and the other using a P2 etch were prepared using adhesive C and they were tested under mode I low-speed impact conditions. The low-speed impact was chosen for the reason that the rate of crack propagation was relatively constant in this test according to the results in Ref. [10] and, therefore, the effect of debond rate on the locus of failure was minimized. Before the tests, each specimen was

mechanically stretched to achieve a high residual stress state [13] (and, consequently, to achieve a high T-stress state) such that alternating crack propagation was observed in the specimen. After failure, post-failure analyses *via* XPS and Auger depth profiling were conducted on the failure surfaces of a typical specimen to identify the locus of failure and the crack propagation trajectory.

The failure surfaces of the typical specimen selected are shown in Figure 6. The T-stress in the specimen was 36 MPa and the crack trajectory alternated between the two interfaces, which can be observed in the side-view photograph. To identify further the locus of failure, both the XPS and Auger depth profile analyses were conducted on representative areas of both sides of the specimen, as schematically shown in Figure 6, and the results are listed in Table V. The XPS results show that the carbon and silicon concentrations on the acetone-wiped adherend surface are lower than on the P2-etched adherend surface, whereas the aluminum and oxygen concentrations are much higher. This trend of the variation of the major element concentrations on the failure surfaces indicates that the locus of failure

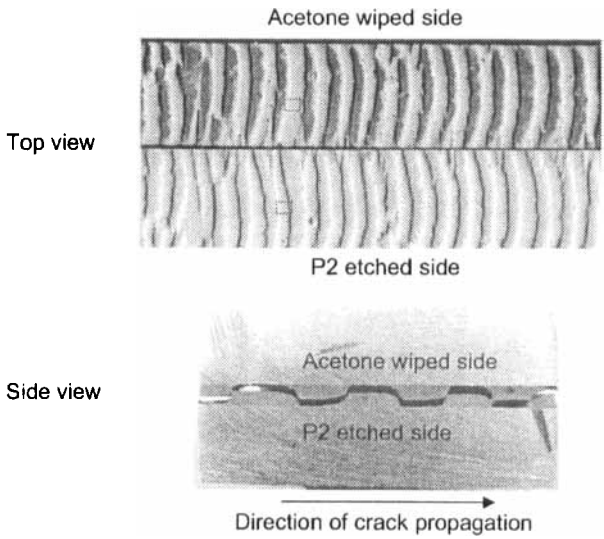

FIGURE 6 The failure surfaces and the crack trajectory of the DCB specimen with asymmetric surface preparation. The ⬚ indicates the areas where XPS and Auger analyses were conducted.

TABLE V The post failure analysis results on the failure surfaces of the DCB specimen with asymmetric surface preparation

Surface	*XPS atomic percentage*					*Film thickness*
treatment	*%C*	*%Al*	*%O*	*%Si*	*%N*	*(μm)*
Acetone	75.8	0.9	17.2	3.8	2.3	0.6 μm
P2	76.7	0.1	16.5	4.5	2.2	1.4 μm

on the acetone-wiped adherend side was more interfacial than on the P2-etched adherend side. The exact locations of the failure on both adherends surfaces were revealed by the Auger depth profile data as shown in the Table V. On the surfaces of the adherend prepared using the acetone wipe, a layer of adhesive film of 0.6 μm thick was detected. However, on the surfaces of the adherend prepared using the P2 etch, the adhesive film detected was much thicker (1.4 μm), which indicated that the failure was more cohesive.

Toughness of the Adhesive and the Directional Stability of Cracks

As pointed out by Pocius [33], the directional stability of cracks is significantly affected by the fracture toughness of adhesive bonds. Using an energy model, Chen and Dillard [12] later analyzed energy flows during crack propagation in adhesively-bonded DCB specimens and predicted that directionally unstable cracks are more unlikely to occur as the fracture toughness of the adhesive bonds increases. To verify the prediction, DCB specimens using adhesive A, B, C and E were prepared. Due to the various levels of rubber concentration in the adhesives, the fracture toughness of the DCB specimens varied with the adhesive. The critical fracture toughnesses measured in the quasi-static tests for the DCB specimens using different adhesives are shown in Figure 7, which indicates that the fracture toughness of the bonds increased significantly with rubber concentration level. After the specimens were prepared, they were subjected to mechanical stretching until plastic deformation occurred in the adherends to achieve various levels of the T-stress in the specimens [13]. The specimens were then tested under low-speed impact loading to achieve a relatively constant debond rate in the tests. After failure, the failure surfaces in each

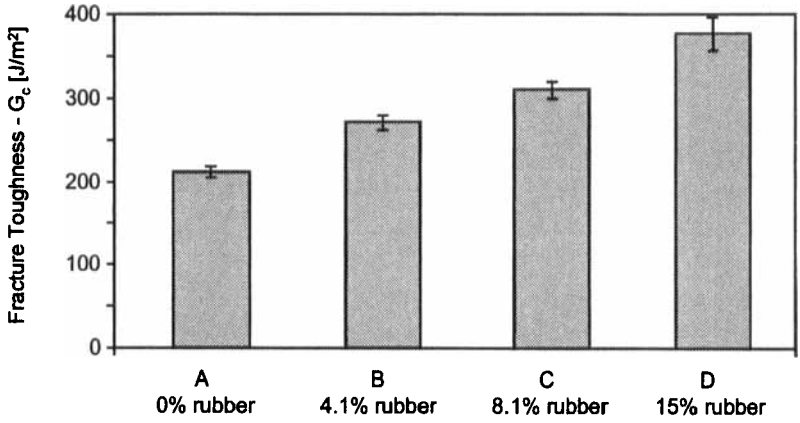

FIGURE 7 The fracture toughness of the DCB specimens using adhesives with different levels of rubber concentrations. Error bars represent ± 1 standard deviation.

specimen were carefully examined to determine crack trajectory and the manner of crack propagation.

Typical failure surfaces observed in as-produced specimens are shown in Figure 8. Specimen (a) was bonded using adhesive A, which

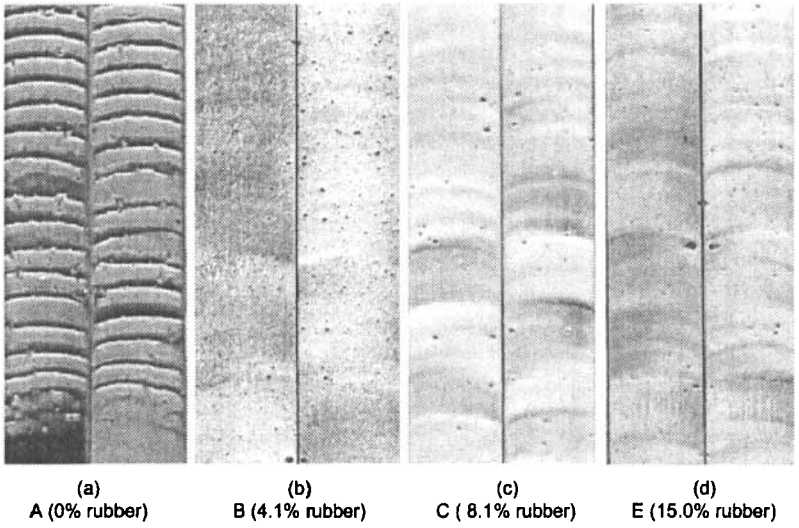

FIGURE 8 The failure surfaces of the as-produced DCB specimens prepared using different adhesives.

contains no rubber toughener and is the most brittle adhesive in the series. The failure surfaces of this specimen revealed an alternating crack trajectory, which indicated that the crack propagation was directionally unstable. As the rubber concentration increased in the adhesive, as in specimens (b), (c) and (d), the failures all appeared to be cohesive with directionally stable crack trajectory. A similar trend had been observed in stretched specimens. All three specimens in Figure 9 contained 1.1% plastic deformation in the adherends and, from specimen (a) to (c), the rubber concentration in the adhesive increased from 4.1% to 15.0%. Examinations of the failure surfaces of these specimens indicate that the crack was directionally unstable in specimen (a) and became more and more stable in specimens (b) and (c). Figures 8 and 9 reveal that the directional stability of the crack is significantly affected by the rubber concentrations in the adhesives. This observation is consistent with the prediction made by Pocius [33] and Chen and Dillard [12]. As the rubber concentration in the adhesive

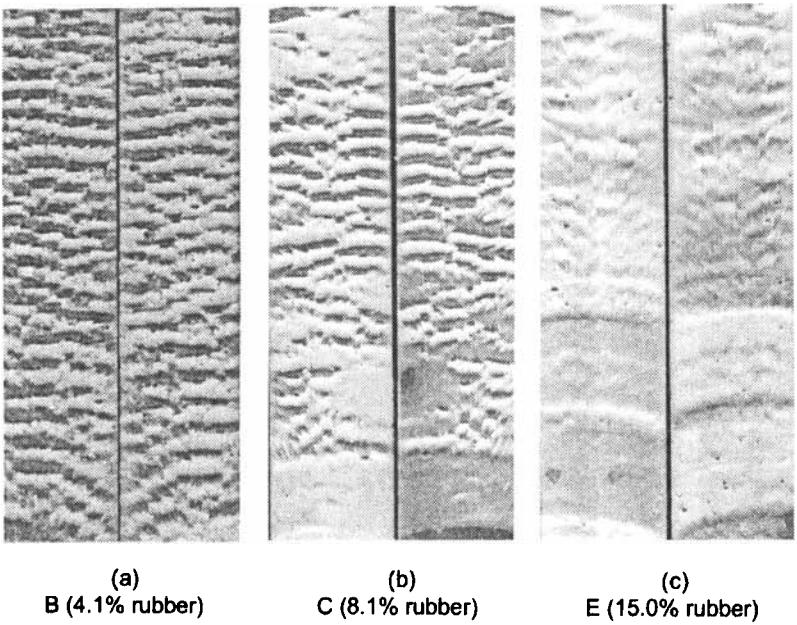

FIGURE 9 The failure surfaces of the DCB specimens prepared using different adhesives. All the specimens contained 1.1% plastic deformation in the adherends.

increases, the fracture toughness of the bonds also increases. Consequently, as indicated by Figure 1, all the curves shift down and the transition from directionally stable cracks to directionally unstable cracks is more unlikely to occur.

CONCLUSIONS AND COMMENTS

This paper investigated the role of materials properties in the crack path selection of adhesively-bonded joints. Through the study, the following conclusions are made:

1. Through a parametric study of directionally unstable cracks in adhesively-bonded joints, the characteristic length of the directionally unstable crack was found to be closely related to the material mismatch of the system: the characteristic length increases as the Dundurs' parameter, α, decreases.
2. The experimental results showed that failure tends to be more interfacial as the fracture mode mixity increases, which verifies the analytical prediction made by applying the criteria of direction of cracking to adhesive bonds. On the other hand, this study also showed that advanced surface preparation methods could improve the interface properties and, consequently, prevent failures at the interfaces. This result demonstrates the effect of interface properties on the locus of failure and verifies that crack path selection in adhesive bonds is a result of interactions between external loads and material properties [9].
3. More advanced surface preparation techniques enhance the adhesion and improve the interface properties. As a result, the rate dependence of the locus of failure can be greatly reduced.
4. By testing the DCB specimens under low-speed impact with one adherend treated with P2 etch and the other treated with acetone wipe, the effect of asymmetric surface preparation on the directionally unstable cracks was studied. The results indicated that due to the asymmetric interface properties, the locus of failure was different on each side of the specimens and the centerline of the directionally unstable crack trajectory was shifted toward the interface of poor adhesion.

5. By testing DCB specimens made using adhesives with various rubber concentrations, the effect of the fracture toughness of the adhesive bonds on the manner of crack propagation was demonstrated. As predicted by Pocius [33] and Chen and Dillard [12], the experimental results showed that as the fracture toughness of the adhesive bonds increases, the transition from the directionally stable cracks to directionally stable cracks is more unlikely to occur.

Acknowledgments

The authors wish to thank the National Science Foundation – Science and Technology Center for High Performance Polymeric Adhesives and Composites #DMR-912004 for supporting this research. The authors would also like to acknowledge the interdisciplinary forum provided by the Center for Adhesive and Sealant Science as well as facilities provided by the Engineering Science and Mechanics Department and the Chemistry Department. We also wish to thank Dr. Charlie Berglund and the Dow Chemical Company for providing the epoxy resin, and Dr. Alphonsus Pocius from the 3M company for helpful comments and suggestions.

References

[1] Cotterell, B. and Rice, J. R., "Slightly curved or kinked cracks", *International J. Fracture* **16**, 155–169 (1980).
[2] Hutchinson, J. W. and Suo, Z., "Mixed mode cracking in layered materials", *Advances in Applied Mechanics* **29**, 63–191 (1992).
[3] Lasson, S. G. and Carlsson, A. J., "Influence of non-singular stress terms and specimen geometry on small-scale yielding at crack tips in elastic–plastic materials", *J. Mech. Phys. Solids* **21**, 263–277 (1973).
[4] Fleck, N. A., Hutchinson, J. W. and Suo, Z., "Crack path selection in a brittle adhesive layer", *Int. J. Solids and Structures* **27**, 1683–1703 (1991).
[5] Williams, M. L., "On the stress distribution at the base of a stationary crack", *J. Applied Mechanics* **24**, 109–114 (1957).
[6] Akisanya, A. R. and Fleck, N. A., "Analysis of a wavy crack in sandwich specimens", *International J. Fracture* **55**, 29–45 (1992).
[7] Akisanya, A. R. and Fleck, N. A., "Brittle fracture of adhesive joints", *International J. Fracture* **58**, 93–114 (1992).
[8] Daghyani, H. R., Ye, L. and Mai, Y. M., "Effect of thermal residual stress on the crack path in adhesively bonded joints", *J. Materials Sci.* **31**, 2523–2529 (1996).
[9] Dillard, D. A., Chen, B., Parvatareddy, H., Lefebvre, D. and Dillard, J. G., "Where does it fail, and what does that mean?", *Proceedings of the 21st Annual Meeting of the Adhesion Society*, Adhesion Society, 1998, pp. 7–9.

[10] Chen, B., Dillard, D. A., Dillard, J. G. and Clark, R. L. Jr., "Crack path selection in adhesively bonded joints: the roles of external loads and specimen geometry", *Int. J. Fracture* (Accepted, to appear in 2001).
[11] Goldstein, R. V. and Salganik, R. L., "Brittle fracture of solids with arbitrary cracks", *International J. Fracture* **10**, 507–523 (1974).
[12] Chen, B. and Dillard, D. A., "Numerical analysis of the directionally unstable crack propagation in adhesively bonded joints", *Int. J. Solids and Structures* (Accepted, to appear in 2001).
[13] Chen, B. and Dillard, D. A., "The effect of the T-stress on the crack path selection in adhesively bonded joints", *Int. J. Adhesion and Adhesives* (Accepted, to appear in 2001).
[14] Wegman, R. F., *Surface preparation techniques for adhesive bonding* (Noyes Publications, Park Ridge, New Jersey, 1989).
[15] Minford, J. D., *Handbook of aluminum bonding technology and data* (Marcel Dekker, Inc., New York, 1993).
[16] Rogers, N. L., In: *Proceedings of the 13th National SAMPE Technical Conference, Society for the Advancement of Material and Process Engineering*, 1981, p. 640.
[17] Brinson, Hal F. Ed., *Engineered materials handbook. Vol. 3, Adhesives and Sealants* (ASM International, The Materials Information Society, Metals Park, OH, 1990).
[18] Chai, H., "A note on crack trajectory in an elastic strip bounded by rigid substrates", *Int. J. Fracture* **32**, 211–213 (1987).
[19] Suga, T., Elssner, E. and Schmander, S., "Composite parameters and mechanical compability of material joints", *J. Composite Materials* **22**, 917–934 (1988).
[20] ABAQUS, Version 5.8, Hibbitt, Karlsson & Sorenson, Inc. (1998).
[21] Franc2D/L: A crack propagation simulator for plane layered structures, Version 1.4, Swenson, D. and James, M., Kansas State University.
[22] Williams, M. L., "The stress around a fault or crack in dissimilar media", *Bulletin of Seismological Society of America* **49**, 199–204 (1959).
[23] Hutchinson, J. W., Mear, M. E. and Rice, J. R., "Crack paralleling an interface between dissimilar materials", *J. Appl. Mechanics* **54**, 828–832 (1987).
[24] Suo, Z. and Hutchinson, J. W., "Sandwich test specimens for measuring interface crack toughness", *Materials Science and Engineering* **A107**, 135–143 (1989).
[25] Hill, D. A., Kelly, P. A., Dai, D. N. and Korsunsky, A. M., *Solution of crack problem, the distributed dislocation technique* (Kluwer Academic Publishers Dordrecht, 1996).
[26] Dattaguru, B., Venkatesha, K. S., Ramamurthy, T. S. and Buchholz, F. G., "Finite element estimates of strain energy release rate components at the tip of an interface crack under mode I loading", *Engineering Fracture Mechanics* **49**, 451–463 (1994).
[27] Vrana, M. A., Dillard, J. G., Ward, T. C., Rakestraw, M. D. and Dillard, D. A., "The influence of curing agent content on the mechanical and adhesive properties of dicyandiamide cured epoxy systems", *J. Adhesion* **55**, 31–42 (1995).
[28] Dillard, D. A., Park, T. G., Zhang, H. and Chen, B., "Measurement of residual stresses and thermal expansion in adhesive bonds", *Proceedings of the 22nd Annual Meeting of the Adhesion Society*, Adhesion Society, 1999, pp. 336–338.
[29] Dillard, D. A., Chen, B., Chang, T. and Lai, Y. H., "Analysis of the notched coating adhesion test", *J. Adhesion* **69**, 99–120 (1999).
[30] Parvatareddy, H. and Dillard, D. A., "Effect of mode mixity on the fracture toughness of Ti6Al-4V/FM-5 adhesive joints", *International J. Fracture* **96**, 215–228 (1999).
[31] Xiao, F., Hui, C. Y. and Kramer, E. J., "Analysis of a mixed mode fracture specimen: the asymmetric double cantilever beam", *J. Materials Science* **28**, 5620–5629 (1993).
[32] Sundararaman, V. and Davidson, B. D., "An unsymmetric double cantilever beam test for interfacial fracture toughness determination", *Int. J. Solids and Structures* **34**, 799–817 (1997).
[33] Pocius, A., Verbal communication (1998).